Title:
A Generalizable Machine Learning Framework for cfDNA based Early Detection of Hepatocellular Carcinoma

Running Head:
Generalizable ML Framework for Early HCC Detection

Authors and Affiliations:
Mythili Subharam, MS
Founder and CEO, OmicXHealth, Inc., San Jose, CA, USA

Ryan Koehler, PhD
Bioinformatics Scientist, VerdAscend Sciences, Portland, Oregon, USA

Tejas Sreedhar
BS Student, UC Berkeley, California, USA

Corresponding Author:
Mythili Subharam
OmicXHealth, Inc.
San Ramon, CA, USA
Email: mythili.subharam@omicxhealth.com

Acknowledgments:
We thank Paul Gaudin and Dr. Elena Tomas Bort for their early contributions to the data preprocessing and feasibility validation phases of this project.

Previous Presentation:
A version of this manuscript was previously posted as a preprint on bioRxiv:
Subharam M, Koehler R. *A Generalizable Machine Learning Model for Early Detection of Hepatocellular Carcinoma Using Bisulfite Sequencing*. bioRxiv. 2025 Jun 9.
https://www.biorxiv.org/content/10.1101/2025.06.09.658649v1

Funding Information/Research Support:

No external funding was received. The research funding was bootstrapped by the corresponding author on behalf of OmicXHealth.

Disclaimers:
None.

ABSTRACT

PURPOSE

Early detection of hepatocellular carcinoma (HCC) is critical for improving patient outcomes, yet current screening tools lack sensitivity and specificity. We developed a generalizable machine learning framework for HCC detection using methylation profiles from bisulfite sequencing across multiple assay platforms and sample types, enabling a "split-and-filter" approach for accurate cancer classification of sequenced samples without requiring assay compatibility or metadata.

PATIENTS AND METHODS

We analyzed 2,426 samples from four publicly available bisulfite sequencing datasets, three from cell-free plasma DNA (cfDNA) assayed by different methods, and one from tissue biopsy samples assayed with whole genome bisulfite sequencing (WGBS). Machine learning models to classify samples as HCC or normal were constructed. Multiple models encompassing different assay and feature sets were investigated, ultimately settling on assay-specific models combined with a meta-classifier as a general framework.

RESULTS

Assay-specific cfDNA models, trained independently on CpG sites from original publications, were evaluated using the biopsy dataset as blind validation. All three assay-specific models (MCTA-Seq, low pass WGBS and MCB-based targeted

sequencing) generalized well to the validation data, with accuracies of 83.5%-100%. Limited feature overlap among cfDNA models precluded creation of a single high-performance model suitable across assays, but overlap allowed a sample routing meta-classifier. Additional models trained on biopsy WGBS samples filtered to cfDNA model features achieved near-perfect accuracy, indicating that relative methylation patterns remained stable across assays and sample types.

CONCLUSION

A generalizable framework for early detection of HCC composed of assay-specific classifiers and a meta-classifier is described. This architecture readily accommodates addition of new assays, supporting WGBS flexibility via feature-matched models and meta-classification, which makes it especially powerful in clinical contexts.

INTRODUCTION

Hepatocellular carcinoma (HCC) is the most common form of primary liver cancer and a leading cause of cancer-related mortality worldwide. Prognosis is closely tied to stage at diagnosis, yet the majority of cases are identified at advanced stages, when curative treatment options are limited. The current standard of care for early HCC surveillance in high-risk patients is ultrasound imaging with or without serum alpha-fetoprotein (AFP) testing, but this offers only modest sensitivity (~65%), particularly for early-stage tumors[7] and obese patients[8]. There is a pressing need for more sensitive, non-invasive detection methods that can identify HCC at an earlier, curable stage.

Liquid biopsy approaches based on cell-free DNA (cfDNA) have shown considerable promise for non-invasive cancer detection. While many commercial platforms focus on detecting somatic mutations, this strategy is poorly suited for early detection in HCC, where tumor-derived DNA often constitutes a small fraction of total cfDNA. Moreover, mutational profiles vary widely across patients and disease stages, making it difficult to train models that capture consistent, generalizable patterns[9,10]. In contrast, epigenetic DNA methylation level alterations are early events in tumorigenesis and tend to occur in conserved regulatory regions across individuals. These patterns are more stable across patients and cancer stages, providing a richer and more consistent signal for machine learning–based classification[11]. Bisulfite sequencing of cfDNA enables single-base resolution of methylation patterns and can be applied in both genome-wide and variously targeted assay formats. Compared to array-based or probe-constrained methods, bisulfite sequencing offers greater sensitivity and flexibility in detecting tumor and tissue-specific epigenetic changes, even in samples with low tumor DNA content, which makes it particularly well suited for early cancer detection[11].

While cfDNA methylation is a promising biomarker class for early cancer detection[1], published models and commercial tests have struggled to generalize beyond their original datasets. For example, the Galleri methylation-based multi-cancer detection test demonstrated high specificity (~99%) but only 16.8% sensitivity in early-stage cancers[15]. We hypothesized that assay-aware machine learning models, trained on biologically grounded methylation features, could achieve high accuracy across different bisulfite sequencing platforms, sample types and patient populations. Use of an ensemble approach, specifically a "mixture of experts" or a "gating network" architecture, might

yield a sensitive and general predictive tool[12].To test this, we developed a modular framework using public cfDNA datasets generated with three distinct bisulfite sequencing assays and evaluated generalizability using an independent tissue-based dataset for blind validation.

METHODS

Data Sources

We analyzed four publicly available bisulfite sequencing datasets representing plasma-derived cfDNA and liver tissue from hepatocellular carcinoma (HCC) patients and healthy controls, each generated using a distinct assay (supplementary **Table S1**). These include: GSE93203, which used targeted bisulfite sequencing of plasma-derived cfDNA targeting methylation-correlated blocks (MCBs) across 467 short genomic regions[4]. These regions were selected based on coordinated methylation patterns associated with HCC, but this small footprint may be poorly sampled by broader sequencing assays; GSE63775, another targeted assay with limited genomic footprint, which used Methylated CpG Tandem Amplification and Sequencing (MCTA-Seq) of plasma-derived cfDNA to enrich for fully methylated CpG islands[2]; PRJCA001372, which used low-depth whole-genome bisulfite sequencing (WGBS) of plasma-derived cfDNA targeting hypomethylated markers[3]; and PRJNA984754, a moderate-depth WGBS dataset of matched HCC and adjacent normal liver tissue biopsy samples[5].

Feature Selection

For each dataset, FASTQ sequencing files were processed through a bioinformatics pipeline using Bismark[16] to compute “beta values”, defined as the ratio of methylated reads to total reads covering a CpG site. All sites with aligned reads were included in beta value calculations. Initial data matrices were created by collecting beta values from all samples at CpG sites previously identified as relevant for HCC detection by the original study authors. These were subsequently filtered to remove CpG sites exhibiting zero variance across samples.

The GSE93203 (MCB) dataset yielded limited CpG coverage when raw FASTQ files were processed through our standard pipeline, with many loci from the original study showing little or no usable signal. We then obtained the original study’s published beta value matrix (n=467 CpGs) and manually mapped the biomarker coordinates described in the paper to genomic locations. These mapped regions were cross-referenced against the 467 CpGs in the matrix, resulting in a final set of 32 CpG sites corresponding to 18 reported biomarker loci.

Model Training and Internal Validation

Because each cfDNA dataset was generated from a different assay, there was minimal overlap in CpG coverage across the datasets. This precluded construction of a high-performance unified model using only shared features. Instead we opted to train three separate machine learning models, using CpG sites selected from the corresponding publications. While the reduced feature set across all models was not adequate for high-performance joint modeling, it nevertheless proved sufficient to

support a meta-classifier for model routing of samples to appropriate assay-specific models.

The XGBoost[18] algorithm is known for its strong performance, especially when handling missing values without requiring imputation[13]. We developed models specific for each explored dataset using this approach. Random Forest classifiers were also evaluated during early testing but consistently underperformed relative to XGBoost, particularly on the more sparse beta value matrices. Internal validation was performed using k-fold cross-validation (K = 5 or 10, based on dataset size), with a default classification threshold of 0.5 unless otherwise noted.

Blind Validation

To assess generalizability, each cfDNA model was applied to the independent PRJNA984754 tissue biopsy dataset, which was filtered to match the selected features of the respective training model. All models were evaluated using k-fold cross-validation and standard performance metrics (accuracy, sensitivity, specificity, and AUC).

Predictions were generated using each trained classifier. For each model, a default classification threshold of 0.5 was initially applied. Where appropriate, thresholds were adjusted by inspecting the distribution of predicted probabilities on the validation set, with the goal of maximizing separation between cancerous and non-cancerous samples. In the case of the PRJCA001372 model, the threshold was raised to improve discrimination and reduce false positives. For the GSE93203 model, no clear threshold achieved adequate separation, leading to application of batch correction prior to classification.

Hybrid Tissue Model Construction

To explore the predictive value of features identified from cfDNA in a biopsy tissue context, another model was trained directly on PRJNA984754. This model used CpG sites selected from the PRJCA001372 (hypomethylated, low depth WGBS) and GSE63775 (hypermethylated, MCTA-Seq) datasets. Three variant subsets were assessed: hypomethylated-only features, hypermethylated-only features, and a combined hybrid model using the top 2,000 sites after filtering. To select the top 2,000 features, an initial XGBoost model was trained on the full filtered feature set, and feature importance scores were extracted. The 2,000 highest-ranking features were then used to train a second, reduced model for performance evaluation. This model's performance was assessed using 3-fold cross-validation.

RESULTS

All models achieved strong internal performance, with mean k-fold cross-validation accuracy of 84%-94%. To assess generalizability, we performed blind validation using an independent tissue biopsy WGBS dataset consisting of 12 matched liver cancer-normal tissue pairs (24 samples total). Model inputs and performance metrics are summarized in **Table 1** (and ROC curves are included as supplementary figures).

Table 1. Model summary.

Model ID	Assay Type	Selected Features	Number of Samples	K-fold Internal Validation Accuracy	Blind Validation (PRJNA984754)	AUC	Sensitivity	Specificity
GSE63775	Targeted MCTA-Seq (cfDNA)	3,988 CpG sites	151	84.1% (avg. 5-fold)	83.3%	0.80	83.3%	83.3%
GSE93203	MCB Targeted Bisulfite (cfDNA)	32 CpG sites	2191	93.5% (avg. 5-fold)	83.3%	0.875	91.7%	75%
PRJCA001372	Low depth WGBS (cfDNA)	3,592 CpG sites	60	88.9% (avg. 5-fold)	100.0% (threshold=0.8)	1.00	100.0%	100.0%
PRJNA984754	WGBS (Biopsy tissue)	Three variants: union (2,000), hypo-only, hyper-only	24	100.0% (3-fold, union@0.7 threshold)	—	—	—	—

1. All models used XGBoost classifiers, which outperformed Random Forest in internal comparisons.
2. “Selected Features” indicates the number of CpG sites retained after filtering and preprocessing.

3. For PRJNA984754, three models were trained using different feature sets:
   Hypo-only: CpG sites selected based on hypomethylation in PRJCA001372
   Hyper-only: CpG sites selected based on hypermethylation in GSE63775
   Union: Top 2,000 combined features from both hypo- and hypermethylated site sets

Model Validation Findings

GSE63775 (MCTA-Seq)

Threshold Used: 0.45 *(see Key Insights for rationale)*

Accuracy on Blind Validation: 83.3%

Key Insights: The CpG site–level model trained on GSE63775 generalized well to the independent PRJNA984754 dataset, achieving high accuracy despite differences in assay type (targeted vs. WGBS) and sample source (cfDNA vs. tissue). While global methylation distributions show broader overlap between cancerous and healthy samples in the validation set (**Figure 1B**), site-level boxplots (**Figure 2A**) reveal strong discriminative power at key CpGs. Clear hypermethylation trends in cancer are preserved across datasets, suggesting that the model's predictive performance is driven by a focused subset of informative CpG sites rather than global patterns.

Beta values in the validation dataset are shifted lower across the board—likely reflecting biological or technical differences between plasma-derived and tissue-derived samples. This required a lower prediction threshold to retain sensitivity. The model, having learned "high beta = cancer," needed a threshold adjustment to correctly identify cancer samples with comparatively lower beta values in the validation set.

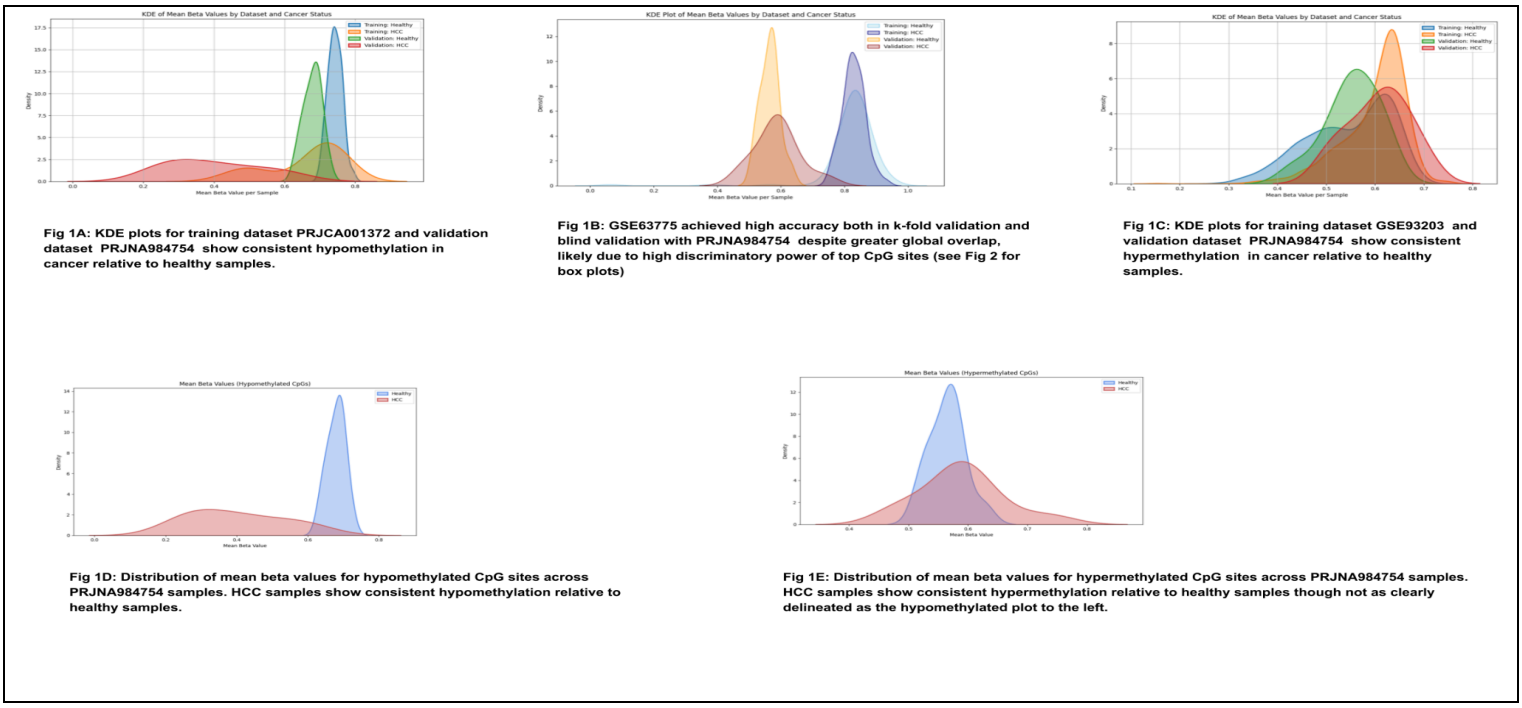

Figure 1. KDE Distribution Plots for Global and Site-Level Methylation Trends Kernel density estimates (KDEs) comparing the distribution of beta values between cancerous and healthy samples.

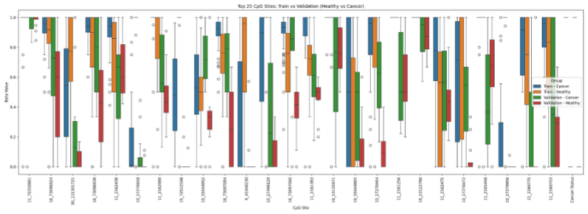

Fig 2A: Boxplot showing beta values at top 25 CpG sites stratified by cancer status and dataset origin for GSE63775 and validation dataset PRJNA984754. **Some distributional drift in beta values/methylation between training and validation sets but the trend (hypermethylation in cancer) is preserved. Outliers present but do not dominate the signal.**

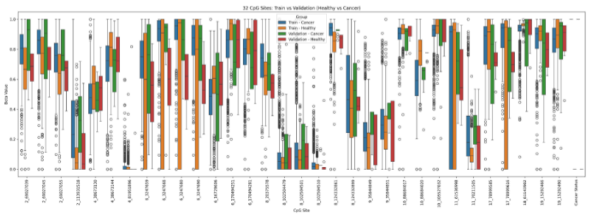

Fig 2B: Beta-value trend comparison for top CpG sites. Boxplots show methylation levels at the 32 selected CpG sites from the GSE93203 model, stratified by dataset (GSE93203 vs. PRJNA984754) and sample class (cancer vs. healthy). Most sites display hypermethylation trends in cancer in both datasets, a strong sign of generalization of methylation patterns across assay types and sample types.

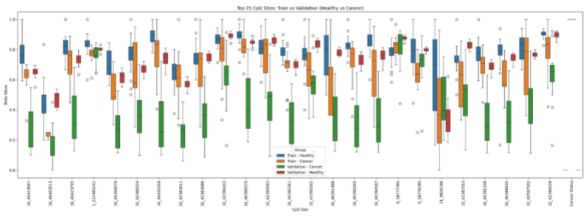

Fig 2C: Top 25 CpG sites selected by the PRJCA001372 model, showing beta value distributions across training and validation datasets. Boxplots represent methylation levels for cancer and healthy samples in both the training dataset (PRJCA001372) and the independent validation dataset (PRJNA984754). The majority of CpG sites display hypomethylation in cancer samples, consistent with known epigenetic patterns in HCC. These patterns are preserved across datasets, supporting the robustness and generalizability of the selected markers.

Figure 2. Boxplot Summary of Methylation Differences Across Training and Validation datasets Boxplots comparing beta values of cancerous and healthy samples at key CpG sites across training and validation datasets.

GSE93203 (MCB-Based Targeted Sequencing)

Threshold Used: 0.5 (after batch correction)

Accuracy on Blind Validation: 83.5%

Key Insights:

The GSE93203 model, trained using a refined set of 32 CpG sites mapped from 18 published biomarkers, achieved strong generalization to the independent PRJNA984754 validation dataset following status-aware batch correction. While earlier

attempts using larger feature sets (e.g., 467 CpGs from the supplementary matrix) and traditional batch correction approaches failed to generalize, restricting the model to biologically validated markers improved both stability and performance.

After applying a cancer status–specific mean shift correction to the methylation beta values—where mean differences between cancerous and non-cancerous samples in the training and validation sets were aligned separately—a clear separation between classes emerged as seen in **Figure 1C**. Fixing the classification threshold at 0.5 post-correction yielded balanced performance across cancerous and non-cancerous tissue samples. This result suggests that although the original assay used targeted enrichment of MCB regions, a focused subset of biologically validated CpG markers can generalize effectively across platforms when normalized appropriately.

PRJCA001372 (Low-Depth WGBS)

Threshold Used: 0.8 *(see Discussion for rationale)*

Accuracy on Blind Validation: 100%

Key Insights:

This model, trained on cfDNA-derived hypomethylated CpGs, achieved perfect classification when tested against PRJNA984754 tissue samples. KDE plots (**Figure 1A**) confirm that cancer samples have lower global beta values, consistent with expected hypomethylation in HCC. The site-level boxplots (**Figure 2C**) reinforce this, showing preserved hypomethylation across training and validation sets.

Although overall methylation levels in the validation dataset were lower for both healthy and cancer samples, cancer-specific hypomethylation remained distinct. A higher

threshold was required to correctly separate the classes, consistent with the model's learning that "low beta = cancer." This underscores the robustness of hypomethylation-based models across different sequencing platforms and sample types.

Standalone Models Trained on PRJNA984754 dataset (WGBS tissue dataset)

Accuracy (3-Fold Cross-Validation):

- **Hypomethylated-only features (from PRJCA001372):** 23/24 correct (threshold = 0.5)
- **Hypermethylated-only features (from GSE63775):** 20/24 correct (threshold = 0.5)
- **Hybrid (hypomethylation + hypermethylation features):** 100% (threshold = 0.7)

Key Insights:

To test whether externally derived feature sets retain predictive power in a purely tissue-derived context, we trained three PRJNA984754-only models using CpG sites selected from the other datasets. KDE plots (**Figure 1D and E**) show meaningful class separation for both hypo- and hypermethylated features. Panel 1D (hypo) reveals clean separation between HCC and healthy samples, while Panel 1E (hyper) shows greater overlap—though cancer samples remain hypermethylated (skewed toward higher beta values).

Boxplots for hypermethylated CpGs (**Figure 2A**) indicate that individual sites maintain strong trends even when global distributions are less distinct. These findings suggest

that while global hypomethylation offers broader signal, select hypermethylated markers can offer high site-level resolution. The hybrid model combining both achieved perfect classification, reinforcing the value of integrating feature types when sequencing depth allows.

ROC curve analysis (see Supplementary section) further illustrates the generalizability of models across datasets. The GSE63775-based model achieved an AUC of 0.9059 on blind validation samples, misclassifying only 4 out of 24. The GSE93203 model yielded an AUC of 0.875 misclassifying 4 out of 24.Notably, the PRJCA001372 model, trained and validated on WGBS-based data, achieved an AUC of 1.0, suggesting near-perfect alignment and underscoring the impact of methodological consistency between training and validation.

Validation Summary

All three cfDNA-based models — PRJCA001372 (low-depth WGBS), GSE63775 (MCTA-Seq), and GSE93203 (MCB-based targeted bisulfite sequencing) — demonstrated strong generalizability to the independent PRJNA984754 tissue WGBS validation set. Although trained on plasma-derived cfDNA data using different sequencing methods and distinct feature sets, each model successfully distinguished cancerous from non-cancerous tissue samples after aligning methylation profiles across datasets. This supports the hypothesis that biologically relevant methylation patterns at carefully selected individual CpG sites are robust to both biospecimen type and sequencing platform.

The GSE93203 model initially struggled during validation. Despite high intra-dataset accuracy (~94%), it misclassified all healthy samples as cancerous when applied directly to the validation set. Ultimately, a refined model restricted to 32 CpG sites that mapped to the originally published markers was constructed. A cancer status–specific mean shift correction was applied to the beta values, achieving stable separation between classes and a prediction accuracy of 83.3%. This result suggests that when focused on a validated subset of biomarkers and normalized appropriately, even assay-specific models can generalize well across platforms.

Prediction thresholds required for accurate classification varied across models due to global shifts in methylation levels in the tissue-derived validation set. As shown in **Figure 2** (Panels A–C), the directionality of cancer-associated methylation shifts remained consistent even when absolute beta values differed, facilitating successful generalization across the three models.

DISCUSSION

This study demonstrates that a generalizable machine learning (ML) framework can accurately detect hepatocellular carcinoma (HCC) using cfDNA methylation data from multiple sequencing platforms. Unlike prior studies that relied on siloed datasets or proprietary assays, our approach integrates platform-specific models within a unified meta-classifier architecture. Each model was trained on biologically relevant CpG markers identified by the original study authors, using conservative feature filtering to balance granularity and generalization. Cross-validation showed strong within-cohort performance, and blind validation using an independent whole-genome bisulfite

sequencing (WGBS) liver tissue dataset confirmed that cfDNA methylation signatures are both biologically robust and technically generalizable.

A key feature of this framework is its flexibility in handling assay heterogeneity. When the sequencing method is known (e.g., WGBS), sample data can be preprocessed into multiple filtered versions—each corresponding to the feature set of a trained model—and passed through all models independently. Final classification is based on the prediction with the highest confidence score, which reflects how well the sample's methylation pattern matches disease-associated features. For example, strong hypomethylation across key sites yields higher confidence from the hypomethylation model. In real-world scenarios where assay metadata may be unavailable, the meta-classifier offers a robust alternative: using a small, shared subset of intersecting CpG features, it routes the sample to the most appropriate model based on methylation signature similarity—enabling accurate predictions without prior knowledge of sequencing modality.

This work also confirms the stability of methylation patterns across cancer stages and sample types. All three training datasets (MCTA-Seq, WGBS, and padlock probe–based assays) included early to late HCC stages, yet each model performed well during cross-validation. The WGBS liver tissue dataset—despite being derived from solid tissue rather than plasma—validated strongly against all three cfDNA-trained models, suggesting that cfDNA and tissue share stable methylation signatures across sequencing methods and clinical contexts.

Another insight was the impact of sequencing technology on model generalizability. Among the three models, the one trained on WGBS achieved the highest accuracy during blind validation, likely reflecting the benefit of matched sequencing platforms between training and test sets. Still, the MCTA-Seq and padlock-based models also performed well despite their differing platforms, underscoring that methylation-based classifiers can generalize across assays when features are biologically meaningful.

We also observed that methylation beta values often shift downward in absolute magnitude between training and validation datasets, likely due to differences in sample type (plasma vs. tissue) and sequencing depth. For the PRJCA001372-trained model, this global downward shift caused all validation samples to appear more hypomethylated than expected. While cancer samples still had lower methylation than controls, all probabilities shifted upward. Raising the classification threshold restored accuracy by separating the classes based on the new distribution. The GSE93203-trained model showed a more extreme mismatch: both cancerous and healthy validation samples fell into the non-cancer methylation range of the training data. Although relative trends were preserved (cancer < healthy), the shift invalidated threshold-based classification. In this case, batch correction was necessary to realign distributions and recover predictive accuracy. These findings suggest that while modest platform shifts can be addressed via threshold tuning, substantial mismatches require explicit harmonization.

CONCLUSION

This study demonstrates the feasibility of a generalizable machine learning framework for early hepatocellular carcinoma (HCC) detection using cfDNA methylation data

derived from diverse bisulfite sequencing platforms. We trained three distinct models using public datasets capturing hypermethylation, hypomethylation, and hybrid signatures, and validated their performance on an independent WGBS liver tissue dataset. All models achieved strong predictive accuracy, with the hypomethylation model reaching 100% accuracy after threshold adjustment.

Because all models operate on CpG-level features, the framework allows flexible routing of individual samples through multiple classifiers based on their methylation profile. This architecture enables scalable and cost-effective deployment across a range of sequencing protocols.

Crucially, the framework is extensible. As emerging cfDNA methylation biomarkers are identified in the literature—such as GJA4 in HBV-associated HCC—they can be incorporated into future iterations of the model without requiring changes to the assay protocol. This adaptability strengthens long-term clinical utility.

Collectively, these findings support the use of a multi-model, meta-classifier–based approach for HCC detection, offering both technical flexibility and biological robustness. Retrospective clinical validation using biobank-derived cfDNA samples is warranted to assess real-world performance and inform potential integration into early cancer screening workflows.

Bibliography and Citations

1. Fu, S., Debes, J.D., Boonstra, A. (2023). DNA methylation markers in the detection of hepatocellular carcinoma. *European Journal of Cancer*, 191, 112960. https://doi.org/10.1016/j.ejca.2023.112960
2. Wen, L., Li, J., Guo, H., et al. (2015). Genome-scale detection of hypermethylated CpG islands in circulating cell-free DNA of hepatocellular carcinoma patients. *Cell Research*, 25(11), 1250-1264. https://doi.org/10.1038/cr.2015.126
3. Zhang, H., Dong, P., Guo, S., et al. (2020). Hypomethylation in HBV integration regions aids non-invasive surveillance to hepatocellular carcinoma by low-pass genome-wide bisulfite sequencing. *BMC Medicine*, 18, 200. https://doi.org/10.1186/s12916-020-01667-x
4. Luo, Y., Zeng, Q., et al. (2017). Characterization of methylation-correlated blocks in hepatocellular carcinoma. *Nature Materials*, Published online October 9, 2017. https://doi.org/10.1038/NMAT4997
5. Zhao, et al. (2023). Comprehensive analysis of DNA methylation patterns for early-stage liver cancer detection using bisulfite sequencing. *Research Square*, Published online June 29, 2023. https://doi.org/10.21203/rs.3.rs-3105819/v1
6. Sun, Y., Liu, X., Zhang, Y., et al. (2025). A liquid biopsy approach detects HCC and identifies GJA4 as a potential biomarker for HBV-HCC via plasma cfDNA methylome profiling. *Clinical Epigenetics*, 17, Article 125. https://doi.org/10.1186/s13148-025-01909-w

7. Tzartzeva, Kristina et al. (2018) Surveillance Imaging and Alpha Fetoprotein for Early Detection of Hepatocellular Carcinoma in Patients With Cirrhosis: A Meta-analysis *Gastroenterology, Volume 154, Issue 6, 1706 - 1718.e1* ***https://doi.org/10.1053/j.gastro.2018.01.064***
8. Esfeh JM, Hajifathalian K, Ansari-Gilani K. Sensitivity of ultrasound in detecting hepatocellular carcinoma in obese patients compared to explant pathology as the gold standard. Clin Mol Hepatol. 2020 Jan;26(1):54-59. doi: 10.3350/cmh.2019.0039. Epub 2019 Nov 15. PMID: 31726817; PMCID: PMC6940490.
9. Lu LC, Hsu CH, Hsu C, Cheng AL. Tumor Heterogeneity in Hepatocellular Carcinoma: Facing the Challenges. Liver Cancer. 2016 Apr;5(2):128-38. doi: 10.1159/000367754. Epub 2016 Mar 17. PMID: 27386431; PMCID: PMC4906428.
10. Fridland S, Choi J, Nam M, Schellenberg SJ, Kim E, Lee G, Yoon N, Chae YK. Assessing tumor heterogeneity: integrating tissue and circulating tumor DNA (ctDNA) analysis in the era of immuno-oncology - blood TMB is not the same as tissue TMB. J Immunother Cancer. 2021 Aug;9(8):e002551. doi: 10.1136/jitc-2021-002551. PMID: 34462324; PMCID: PMC8407207.
11. Li L, Sun Y. Circulating tumor DNA methylation detection as biomarker and its application in tumor liquid biopsy: advances and challenges. MedComm (2020). 2024 Nov 9;5(11):e766. doi: 10.1002/mco2.766. PMID: 39525954; PMCID: PMC11550092.
12. Shazeer, Noam & Mirhoseini, Azalia & Maziarz, Krzysztof & Davis, Andy & Le, Quoc & Hinton, Geoffrey & Dean, Jeff. (2017). Outrageously Large Neural

Networks: The Sparsely-Gated Mixture-of-Experts Layer. 10.48550/arXiv.1701.06538.

13. M. A. Latief, A. Bustamam and T. Siswantining, "Performance Evaluation XGBoost in Handling Missing Value on Classification of Hepatocellular Carcinoma Gene Expression Data," 2020 4th International Conference on Informatics and Computational Sciences (ICICoS), Semarang, Indonesia, 2020, pp. 1-6, doi: 10.1109/ICICoS51170.2020.9299012. keywords: {Performance evaluation;Sensitivity;Computational modeling;Biological system modeling;Data models;Gene expression;Tuning;cross-validation;grid search;KNN imputation mean imputation;XGBoost},
14. Shen J, Wang S, Zhang YJ, Kappil M, Wu HC, Kibriya MG, Wang Q, Jasmine F, Ahsan H, Lee PH, Yu MW, Chen CJ, Santella RM. Genome-wide DNA methylation profiles in hepatocellular carcinoma. Hepatology. 2012 Jun;55(6):1799-808. doi: 10.1002/hep.25569. Epub 2012 Apr 24. PMID: 22234943; PMCID: PMC3330167.
15. Klein EA, Richards D, et al. Clinical validation of a targeted methylation-based multi-cancer early detection test using an independent validation set. *Annals of Oncology*, Volume 32, Issue 9, September 2021, Pages 1167–1177. https://doi.org/10.1016/j.annonc.2021.05.806
16. Krueger F, Andrews SR**.** *Bismark: a flexible aligner and methylation caller for Bisulfite-Seq applications.* Bioinformatics, 2011 Jun 1;27(11):1571–1572. https://doi.org/10.1093/bioinformatics/btr167

17. Johnson, W. E., Li, C., & Rabinovic, A. (2007). Adjusting batch effects in microarray expression data using empirical Bayes methods. *Biostatistics*, **8**(1), 118–127. https://doi.org/10.1093/biostatistics/kxj037

18. Chen, T., & Guestrin, C. (2016). XGBoost: A scalable tree boosting system. *Proceedings of the 22nd ACM SIGKDD Conference on Knowledge Discovery and Data Mining*, 785–794. https://doi.org/10.1145/2939672.2939785